

THE CHEMICAL COMPOSITION OF SERPENTINE/CHLORITE IN THE TUSCALOOSA FORMATION, UNITED STATES GULF COAST: EDX vs. XRD DETERMINATIONS, IMPLICATIONS FOR MINERALOGIC REACTIONS AND THE ORIGIN OF ANATASE

P. C. RYAN† AND R. C. REYNOLDS, JR.

Department of Earth Sciences, Dartmouth College, Hanover, New Hampshire 03755

Abstract—The chemical composition of mixed-layer serpentine/chlorite (Sp/Ch) in Tuscaloosa Formation sandstone was analyzed by energy dispersive X-ray spectroscopy (EDX) in the scanning electron microscope (SEM) and by X-ray diffraction (XRD). EDX results indicate little depth-controlled variation in composition, whereas XRD results suggest distinct decreases in octahedral Fe and tetrahedral Al. XRD-determined compositions appear to be erroneous and actually reflect progressive changes in Sp/Ch unit-cell dimensions caused by polytype transformations of *Ibb* layers to *Iaa* layers in a mixed-layer *Ibb/Iaa* polytype. The relative lack of variation in Sp/Ch composition, especially when compared to other studies of chlorite minerals over similar temperature ranges, is attributed to a reaction mechanism whereby mineralogic transformations (serpentine layers to chlorite layers and *Ibb* layers to *Iaa* layers) occur on a layer-by-layer basis within coherent crystallites, rather than by dissolution-precipitation crystal growth.

The lack of titanium in chlorite minerals is attributed to high levels of octahedral Al^{3+} that prohibit inclusion of the highly charged Ti^{4+} in the octahedral sheet. Anatase (TiO_2) in the Tuscaloosa Formation apparently formed when Ti was liberated during crystallization of Sp/Ch following the breakdown of a Ti-bearing precursor (detrital ultramafic clasts and/or odinite). Odinite, an Fe-rich 7-Å phyllosilicate that forms in some shallow marine sands, apparently existed as a short-lived, poorly crystallized intermediary between dissolution of the ultramafic clasts and formation of Sp/Ch.

Key Words—Anatase, Chemical Composition, Diagenesis, Sandstone, Serpentine/Chlorite, Tuscaloosa Formation.

INTRODUCTION

The accurate determination of chemical composition is essential in examining the relationships among polytypism, mixed layering and diagenetic grade in chlorite and related mixed-layer minerals (such as Sp/Ch and corrensite). In this paper, which is based on a study of authigenic Sp/Ch in the Tuscaloosa Formation, we 1) compare Sp/Ch compositions determined by XRD with those determined by SEM/EDX, 2) address the effect of changing polytypism on XRD-determined compositions, 3) discuss the consistent nature of Sp/Ch chemical composition and 4) address the lack of Ti in chlorite minerals and the presence of anatase in Tuscaloosa Formation sandstone.

Determination of chlorite chemical composition by wet chemical methods and the electron microprobe is often complicated by contamination from other phases such as quartz, illite/smectite, kaolin, anatase and hematite (Curtis et al. 1984; Whittle 1986; Hillier and Velde 1991). To avoid contamination problems, *d*-spacings and peak intensities determined by XRD have been used to estimate chlorite composition (von Engelhardt 1942; Shirozu 1958; Brindley 1961; Kopezhinskas 1965; Bailey 1972; Walker et al. 1988; Chagnon and Desjardins 1991). However, Bailey

(1972) noted that most of the *d*-spacing equations were determined from studies of the *Iib* polytype, and he implied that application of these equations to type-I polytypes could result in errors. Whittle (1986) compared TEM/EDX and XRD compositional analyses and indicated that, for chlorite of the *Ibb* polytype, the XRD method gives erroneously high tetrahedral Al and low octahedral Fe values. Bailey (1972) indicated that using the relative intensities of chlorite basal reflections is a less accurate estimate of octahedral Fe content than the *d*-spacing method, but the basal intensities can be useful in estimating Fe distribution between the octahedral sheet in the 2:1 layer (talclike) and the octahedral sheet in the hydroxide interlayer (brucite-like) (Walker et al. 1988; Chagnon and Desjardins 1991).

Anatase, a polymorph of TiO_2 , is a common trace mineral in sedimentary rocks, but its origin is uncertain. In Lower Tuscaloosa Formation sandstone, anatase content is abnormally high, as is shown by its presence in XRD patterns (Figure 1) and an ICP chemical analysis (performed by X-ral Laboratories, Ontario, Canada), which indicated that TiO_2 comprised 8% by weight of the $<2 \mu m$ fraction (e.s.d.) of sandstone from 3878 m burial depth. Yoneyama et al. (1989) showed that anatase can occur as pillars in smectite interlayers, and Yau et al. (1987) implied that anatase forms during the smectite-to-illite transformation.

† Current address: Environmental Science Program, Salish-Kootenai College, Pablo, Montana 59855.

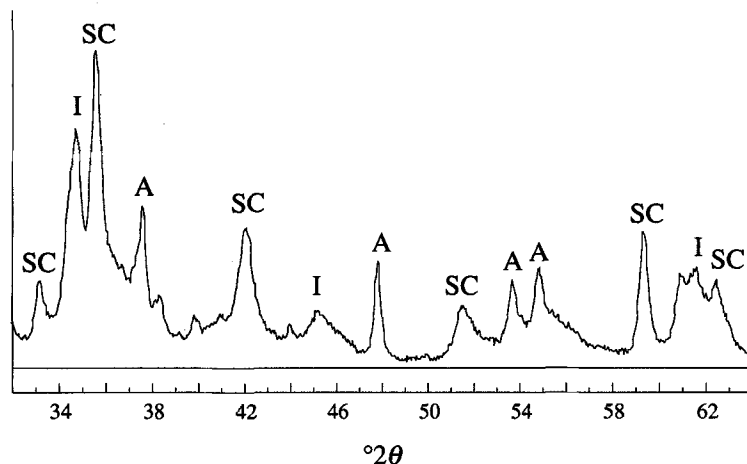


Figure 1. X-ray diffraction pattern of the $<0.5 \mu\text{m}$ fraction of Tuscaloosa Formation sandstone (1937 m burial depth). SC = mixed-layer serpentine/chlorite, I = illite, A = anatase.

Chemical compositions published by Eggleton and Banfield (1985), Al-Dahan and Morad (1986), Newman (1987), Brigatti et al. (1991) and Deer et al. (1992) show that biotite, pyroxene and amphibole can contain up to 10% TiO_2 , but chlorite contains little or none (Curtis et al. 1984; Whittle 1986; Hillier and Velde 1991; Jiang et al. 1994). Eggleton and Banfield (1985) indicated that Ti is liberated during the retrograde metamorphic reaction of granitic biotite to chlorite, suggesting that anatase could form in sedimentary rocks during the alteration of detrital mafic minerals to chlorite or Sp/Ch.

GEOLOGIC SETTING

The Tuscaloosa Formation was deposited in deltaic and nearshore shallow marine environments in the U.S. Gulf Coast basin during Late Cretaceous (Cenomanian) time (Stancliffe and Adams 1986; Hogg 1988). It outcrops along an east-striking trend in Alabama and adjacent states and dips approximately 1° to the south, reaching a maximum burial depth of 6800 m in the subsurface of southern Louisiana (Stancliffe and Adams 1986), where it passes basinward into shale. Authigenic Sp/Ch is abundant, commonly occurring as pore-linings, pore-fillings, peloids, replacements and infillings (Thomsen 1982; Ryan and Reynolds 1996). Most studies on this topic have indicated that the formation of chloritic pore-linings during early diagenesis inhibits quartz nucleation and growth (Heald and Anderegg 1960; Pittman and Lumsden 1968; Wiygul and Young 1987; Ehrenberg 1993), a process that has resulted in abnormally high primary porosity ($>20\%$) at depths as great as 6600 m in Tuscaloosa Formation sandstone (Thomsen 1982). Numerous petrographic previous studies, including those by Thomsen (1982), Hearne and Lock (1985), Hamlin and Cameron (1987) and Wiygul and Young (1987), have published SEM photomicrographs of Tuscaloosa Formation Sp/Ch.

MINERALOGY OF Sp/Ch IN THE TUSCALOOSA FORMATION

Ryan and Reynolds (1996) used XRD and SEM/EDX to determine the origin, structure and diagenesis of pore-lining chloritic material in Tuscaloosa Formation sandstone. The chloritic material in the Tuscaloosa Formation consists of randomly interstratified 7-Å serpentine layers and 14-Å chlorite layers, and the proportion of serpentine layers in the mixed-layer serpentine/chlorite (Sp/Ch) decreases from 21% to 1% with increasing burial depth over a 4300-m interval (Figure 2a), indicating that serpentine layers transform to chlorite layers during diagenesis. The Sp/Ch occurs as type-I chlorite characterized by randomly interstratified *Ibb* and *Iaa* layers. The proportion of the *Ibb* and *Iaa* polytype layers also varies with burial depth, progressively changing from essentially pure *Ibb* in shallow samples (<2000 m) to mixed-layer *Ibb/Iaa* with up to 51% *Iaa* layers at depths >4500 m (Figure 2b; Ryan and Reynolds 1996). XRD data indicate that there is little or no variation in crystallite thickness (c^* direction) (Ryan and Reynolds 1996), and SEM photomicrographs indicate that pore-lining Sp/Ch occurs as hexagonal crystals of 7–10 μm diameter, the size of which does not vary as a function of grade (Thomsen 1982). The Sp/Ch originated as odinite (Ryan and Reynolds 1996), an Fe-rich 7-Å mineral that forms at the sediment-seawater interface in shallow, tropical marine sediments (Bailey 1988a; Odin 1990). The odinite formed during very early diagenesis following the dissolution of detrital ultramafic rock fragments (Thomsen 1982) and transformed to Sp/Ch during very early diagenesis (Ryan and Reynolds 1996). The Sp/Ch primarily occurs as pore-linings with lesser amounts of peloids, pore-fillings, infillings and replacements of biotite grains.

MATERIALS AND METHODS

Specimens analyzed in this study are sandstone cores sampled from 6 drillholes that penetrated the Lower Tuscaloosa Formation at the following burial depths: 1937, 2732, 3878, 4054, 4554 and 5470 m (Figure 3). Current burial temperatures range from 85 to 165 °C (Alford 1983; Ryan 1994). These specimens, provided by David R. Pevear of Exxon Production Research Company (Houston, Texas), were selected because they represent the full range of polytypism and interstratified serpentine content as analyzed by Ryan and Reynolds (1996). The specimens from 1937, 3878, 4554 and 5470 m burial depth are medium-grained, friable sandstone, whereas the specimens from 2732 and 4054 m are fine-grained and well-cemented by quartz.

Cores used in XRD analyses were washed in distilled water to remove drilling mud, gently crushed in an iron mortar and pestle without grinding (Bailey 1988b), immersed in distilled water and agitated for 12 h in a sample shaker. The <0.5 µm and 0.5–2 µm fractions (e.s.d.) were then removed from bulk powders by timed centrifugation and analyzed for mixed layering of serpentine and chlorite layers (Reynolds et al. 1992), bulk mineral content, peak position and Sp/Ch polytypism (Ryan and Reynolds 1996). The XRD data were obtained using an automated Siemens D-500 X-ray diffractometer with CuKα radiation, a graphite monochromator and a Databox microcomputer. In determining mixed layering and polytypism, step size was 0.05 °2θ and count times varied from 5 s (mixed-layer analysis) to 20 s (polytype analysis) per step. The Sp/Ch $d(00,10)$ values were obtained from oriented mounts using 0.02 °2θ steps and 40-s counts. The XRD analyses were performed on a total of 19 specimens for the purpose of determining mixed layering, on 14 samples for the purpose of determining polytypism and on 6 samples for determining $d(00,10)$.

Estimation of Tetrahedral Al by XRD

The XRD estimation of tetrahedral Al in chlorite is based on the observation that substitution of Al for Si in the tetrahedral sheet decreases $d(001)$. Brindley (1961) derived an equation for determining tetrahedral Al:

$$d(001) = 14.55 \text{ \AA} - 0.29x \quad [1]$$

where x is the number of Al atoms per 4 tetrahedral sites. This equation was chosen to estimate tetrahedral Al content in this study because it is based on d -spacings determined from *Ibb* chlorite, the polytype found in Sp/Ch from the shallow (<2000 m) Tuscaloosa Formation. The *Ibb* polytype also occurs in deeper samples, but it is randomly interstratified with the *Iaa* polytype (Ryan and Reynolds 1996).

Oriented powder mounts were prepared by concentrating 50–100 mg of clay in distilled water and dropping the clay slurry onto 2.8-cm by 4.7-cm glass slides. Values of $d(001)$ were determined from oriented mounts by measuring d -spacings of the Sp/Ch 00,10 peak and multiplying by 10. The 2θ position of the anatase 204 peak was analyzed to ensure that determinations of $d(00,10)$ were not compromised by errors in sample position. In addition, $d(001)$ of the pure end-member *Iaa* polytype was estimated by calculating NEWMOD diffraction patterns (Reynolds 1985) of the 00,10 peak for a mixed-layer mineral where one of the components was *Ibb* with $d(001) = 14.11 \text{ \AA}$ (based on analytical measurements of *Ibb*), and the other component was *Iaa*. The d -spacing of the *Iaa* was altered until NEWMOD-calculated peak breadths and peak positions matched those found in analytical 00,10 peaks. The resulting value for $d(001)$ of the *Iaa* layers is 14.31 Å.

Estimation of Octahedral Fe by XRD

Substitution of the relatively large Fe(II) ion for Mg or Al in the octahedral sheet causes expansion of the a and b cell dimensions and is reflected in $d(060)$ and $d(200)$. Accordingly, von Engelhardt (1942), Shirozu (1958) and Kepezhinskas (1965) derived equations relating octahedral composition and the b dimension as determined from $d(060)$. All of the equations used in the estimation of octahedral Fe appear to have been determined from analyses of the *I1b* polytype. The technique of SEM/EDX is not able to differentiate between Fe(II) and Fe(III), so we used the equation of von Engelhardt (1942), which does not discriminate between Fe(II) and Fe(III), to estimate octahedral Fe content:

$$b = 9.22 \text{ \AA} + 0.028 \text{ Fe}^{\text{II}} \quad [2]$$

where Fe^{II} is the number of Fe atoms per 3 octahedral sites. All Fe is assumed to be Fe(II). The b dimension was determined directly from $d(060)$ and verified by measuring $d(200)$, where $b = a\sqrt{3}$, assuming a monoclinic angle of 97.1° (Bailey 1988b). The d -spacings used to estimate octahedral Fe were obtained from random powder mounts prepared by freeze-drying clay solutions and packing the freeze-dried powders into side-load sample holders (Reynolds et al. 1992). Accuracy of peak position measurements were verified by also analyzing the positions of the anatase 004, 200, 105 and 211 peaks (2.38, 1.89, 1.70 and 1.67 Å). Interfering peaks from anatase, illite and kaolin were removed by differential XRD (Schulze 1982; Ryan and Reynolds 1996).

Distribution of Octahedral Fe

The distribution of Fe between the interlayer hydroxide octahedral sheet and the 2:1 layer octahedral sheet was determined by comparing the intensities of

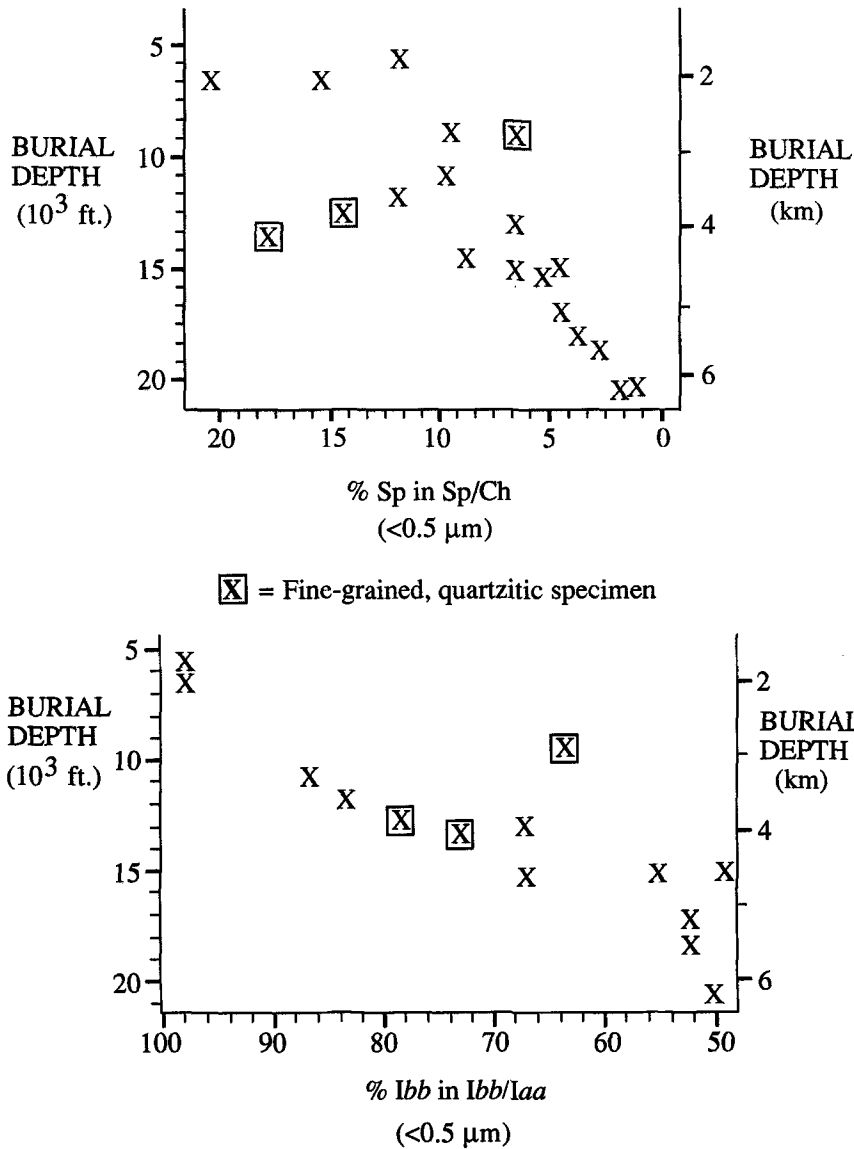


Figure 2a. Relationship between burial depth and % serpentine layers in mixed-layer serpentine/chlorite, $<0.5 \mu\text{m}$ fraction. Boxes indicate fine-grained, well-cemented sandstone specimens. All others are medium-grained, friable sandstones (Ryan and Reynolds 1996).

Figure 2b. Relationship between burial depth and % Ibb layers in mixed-layer Ibb/laa polytype, $<0.5 \mu\text{m}$ fraction. Boxes indicate fine-grained, well-cemented sandstone specimens. All others are medium-grained, friable sandstones (Ryan and Reynolds 1996).

the Sp/Ch 001 and 003 peaks. The NEWMOD calculations show that, for chlorite with no interstratified serpentine layers and symmetrical Fe distribution, the intensities of the 001 and 003 peaks are equal (Reynolds 1985). However, in mixed-layer serpentine/chlorite, the intensity ratio of the 001:003 peaks also varies according to the amount of interstratified serpentine (the 001:003 intensity ratio increases with increasing serpentine). Thus, in order to determine octahedral Fe distribution, analytically determined serpentine con-

tents (Figure 2a) were used as input parameters and Fe distribution was adjusted until the 001:003 intensity ratios of the sample XRD pattern and the NEWMOD-calculated model were equal.

SEM/EDX Determination of Sp/Ch Composition

The chemical composition of Sp/Ch was determined by EDX spot analysis. Between 8 and 11 compositions were determined for each sample, representing all observed Sp/Ch textures (pore-linings, peloids, infillings,

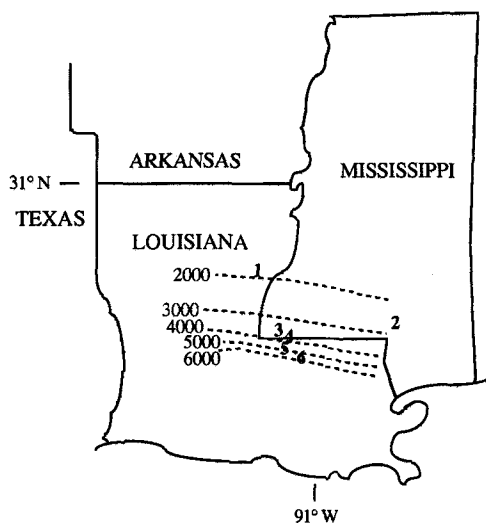


Figure 3. Locations of core samples analyzed in this study. Dotted lines indicate burial depth isopachs in meters, and numbers correspond to cores sampled from the following depths: 1 = 1937 m, 2 = 2732 m, 3 = 3878 m, 4 = 4054 m, 5 = 4554 m, 6 = 5470 m.

pore-fillings, replacements). Polished thin sections were carbon-coated and examined in a Zeiss DSM 962 SEM equipped with an EDX analysis system at the Dartmouth College Electron Microscope Laboratory. Standards were pure oxides for every element except Na, which was an Na-feldspar. Biotite and a granite glass were also analyzed as secondary standards to check reliability. The accelerating voltage was 15 kV, the beam current was 6 nA, spot size was 1–2 μm and the counting time was 100 s per analysis.

Errors and contamination in SEM/EDX compositional analyses most often arise when 1) the electron beam, which is approximately 1–2 μm in diameter (personal communication, Dr. Charles Daghljan, Dartmouth College electron microscope laboratory), interacts with adjacent phases and 2) the beam penetrates through the sought-after mineral and encounters other phases. The diameter of the electron beam was much smaller than the thickness of Sp/Ch pore-linings (5–10 μm) and peloids and infillings (25 to 50 μm across) analyzed in this study, and while we are confident that our EDX analyses are relatively free of contamination from other minerals, intergrowths of authigenic minerals such as illite, kaolin, hematite, anatase and quartz can contaminate analyses (Whittle 1986; Hillier and Velde 1991; Jiang et al. 1994). To avoid contamination from intergrown illite, we discarded analyses with >0.5% K_2O . Contamination from kaolin, quartz and hematite is harder to detect than illite contamination. However, the relatively consistent nature of the EDX analyses argues against significant contamination, although slight variations in Fe content could be due to the presence of hematite.

Samples were analyzed for FeO , MgO , Al_2O_3 , SiO_2 , MnO , K_2O , Na_2O , CaO , TiO_2 and P_2O_5 , and analyses were normalized to a chlorite unit cell with $\text{O}_{10}(\text{OH})_8$. Na_2O and CaO occur only in traces in the samples analyzed (≤ 2 s.d.) and are not included in Sp/Ch compositions because of the minor amounts present and the likelihood that they occur as halite and carbonate (halite and carbonate were detected by XRD and/or thin-section analysis in most samples). Ti and P are also not included in Sp/Ch compositions because they also comprise only traces of most of the samples analyzed (both are typically less than the accuracy of the measurement), and they probably occur in accessory phases such as anatase and apatite (Iijima and Matsumoto 1982; Li and Peacor 1993). However, in some samples TiO_2 content is high, so wt% TiO_2 is listed separately adjacent to Sp/Ch structural formulas where values are greater than 0.3%.

Identification of Anatase

Anatase was identified by the presence of sharp peaks at 3.52, 2.38, 1.89, 1.70 and 1.67 \AA in XRD patterns.

RESULTS

The EDX results are given in Table 1 as oxide percents and in Table 2 as Sp/Ch structural formulas. The XRD-determined compositions are given in Table 3, where they are compared with EDX results.

SEM/EDX Analyses

The SEM/EDX analyses show that there is little variation in Sp/Ch composition (Table 2; Figure 4). The mean chemical composition, mineralogy and diagenetic temperature range of Tuscaloosa Formation Sp/Ch are similar to chlorite and Sp/Ch examined by McDowell and Elders (1980), Jähren and Aagaard (1989), Hillier and Velde (1991) and Jähren and Aagaard (1992), but Tuscaloosa Formation Sp/Ch differs significantly from these previously described diagenetic chlorites in its restricted range of chemical composition and in its virtual lack of temperature-dependent compositional variation. The most notable differences in Sp/Ch composition occur among different textures, particularly in some of the shallow and intermediate depth samples (<4000 m), where Sp/Ch occurring as infillings contains 15 to 20% more Fe than the average of other morphologies (such as peloids, pore-linings and pore-fillings).

High amounts of TiO_2 at 1937 m (1.05%) and 2732 m (1.31%) and the elevated TiO_2 value at 3878 m (0.36%) are attributed to intergrowths of anatase and Sp/Ch in pore space. The anomalously high TiO_2 values were primarily detected in analyses of pore-fillings, infillings and peloids (Table 2). Pore-linings typically contained no TiO_2 , and in the few cases where

Table 1. SEM/EDX analyses (wt%) and structural formulas of Sp/Ch. *N* = number of analyses.

	1937 m (<i>N</i> = 9)	2732 m (<i>N</i> = 7)	3878 m (<i>N</i> = 11)	4054 m (<i>N</i> = 9)	4554 m (<i>N</i> = 8)	5470 m (<i>N</i> = 8)
SiO ₂	8.99 ± 0.10	16.02 ± 0.14	16.71 ± 0.13	17.56 ± 0.13	16.58 ± 0.15	18.82 ± 0.14
Al ₂ O ₃	7.50 ± 0.08	12.70 ± 0.10	13.33 ± 0.10	14.85 ± 0.12	12.63 ± 0.10	16.60 ± 0.13
FeO	11.76 ± 0.20	22.74 ± 0.29	21.92 ± 0.22	25.69 ± 0.25	22.50 ± 0.26	23.92 ± 0.26
MgO	1.49 ± 0.06	2.35 ± 0.07	3.89 ± 0.09	3.25 ± 0.08	3.82 ± 0.08	4.84 ± 0.09
MnO	0.05 ± 0.07	0.05 ± 0.07	0.06 ± 0.09	0.09 ± 0.10	0.08 ± 0.11	0.05 ± 0.10
TiO ₂	1.05†	1.31†	0.36†	0.10 ± 0.06	0.08 ± 0.07	0.07 ± 0.06
K ₂ O	0.05 ± 0.07	0.23 ± 0.05	0.08 ± 0.09	0.05 ± 0.07	0.01 ± 0.05	0.04 ± 0.06
Na ₂ O	0.13 ± 0.07	0.16 ± 0.06	0.29 ± 0.08	0.26 ± 0.08	0.15 ± 0.07	0.31 ± 0.08
CaO	0.11 ± 0.05	0.20 ± 0.06	0.14 ± 0.05	0.25 ± 0.07	0.25 ± 0.07	0.14 ± 0.05
P ₂ O ₅	0.05 ± 0.08	0.07 ± 0.07	0.07 ± 0.08	0.14 ± 0.10	0.12 ± 0.08	0.08 ± 0.09
Total	31.19	55.83	56.85	62.23	56.22	64.86
Si	2.93	2.87	2.91	2.80	2.89	2.82
Al ^{IV}	1.07	1.13	1.09	1.20	1.11	1.18
Al ^{VI}	1.78	1.56	1.58	1.60	1.51	1.72
Fe	3.14	3.57	3.18	3.43	3.31	2.98
Mg	0.72	0.66	1.00	0.77	0.98	1.05
Sum (VI)	5.64	5.79	5.76	5.80	5.80	5.75

† Analytical uncertainty of TiO₂ from individual spot analyses is approximately ± 0.08. However, due to widely varied values for wt% TiO₂, cumulative uncertainty is not presented.

TiO₂ was detected, it was located in the outermost fringes of the pore-lining.

All of the Sp/Ch samples analyzed are Fe-rich, with about half of the octahedral sites occupied by Fe. Fe distribution is somewhat asymmetrical, with approximately 12–21% more Fe in 2:1 layer octahedral sheets than interlayer octahedral sheets. Classified by composition, the Sp/Ch specimens are chamositic (Foster 1962), and they are compositionally similar to authigenic chlorites from North Sea sandstones analyzed by Jahren and Aagaard (1992) and Fe-rich pore-lining Sp/Ch from numerous localities reported by Hillier (1994).

Octahedral occupancy ranges from 5.64 to 5.80, less than the ideal total of 6 for a trioctahedral chlorite mineral, and octahedral Al exceeds tetrahedral Al by 30 to 60%. This is consistent with the findings of Foster (1962), who showed that when chlorite contains excess tetrahedral Al (over tetrahedral Al), the total octahedral occupancy is less than the idealized 6 by ½ of the excess octahedral Al. Octahedral vacancies have also been observed in diagenetic chlorite studied by TEM (Whittle 1986; Jahren and Aagaard 1992) and the electron microprobe (EMP) (Hillier and Velde 1991). There appears to be no correlation between octahedral vacancies and burial depth in Tuscaloosa Formation Sp/Ch.

Oxide totals are less than the expected 85–88% for chlorite with an O₁₀(OH)₈ unit cell, a problem commonly associated with diagenetic chlorite and mixed-layer chlorite minerals (such as Sp/Ch and corrensite). Hillier (1994), when confronted with the same problem in EMP analyses, compared a standard metamorphic chlorite (CCa-1, available from the Clay Minerals Society) prepared as a polished section to the same

specimen prepared as a polished 2–5-µm powder and epoxy resin mixture. The mean oxide total for the polished section was within the expected range (86%), whereas the mean oxide total for the epoxy-powder section was far lower (54%), with many totals between 20 and 50%. Dispersion about the mean was greater for the low oxide data, but the average structural formulas obtained from the polished section and the epoxy section were nearly identical, implying that analyses with low oxide totals are reliable but may contain greater deviations about the mean.

Standard deviations associated with SEM/EDX analyses of Sp/Ch in this study were generally low: 0.8 to 1.1% for Si and Al, 1.0 to 1.5% for Fe and 1.9 to 4.3% for Mg. As expected, analytical errors were greatest for Sp/Ch from 1937 m, where oxide totals were much less than in deeper samples. The low oxide values in the shallowest sample are attributed to greater microporosity between Sp/Ch crystals that is not so pronounced at greater depths.

XRD-Determined Compositions

The XRD spacings show distinct trends in both octahedral Fe and tetrahedral Al (Table 3). Between 1937 m and 5470 m, *d*(060) decreases from 1.556 to 1.549 Å, correlating to a decrease in octahedral Fe from 4.14 to 2.64 (per 6 sites). Over the same interval, *d*(001) increases from 14.11 to 14.16 Å, indicating a decrease in tetrahedral Al from 1.52 to 1.34. The trend of decreasing Al with depth is particularly interesting because it is the opposite of the trend commonly reported for diagenetic chlorites (Hillier and Velde 1991; Jahren and Aagaard 1992; de Caritat et al. 1993).

Table 2. Individual structural formulae of Sp/Ch as determined by SEM/EDX. Particle morphology is indicated by the following symbols: PF = pore-filling, PEL = peloid, INF = infilling, GC = grain-coating/pore-lining, RPL = replacement of biotite grain, ave = average composition for that core specimen. TiO₂ is also shown where it comprises >0.3% (by wt).

EDX composition	Texture	% TiO ₂
1937 m Burial depth		
(Fe _{3.02} Mg _{0.74} Al _{1.86})(Si _{2.90} Al _{1.10})O ₁₀ (OH) ₈	PF	0.64
(Fe _{3.07} Mg _{0.75} Al _{1.82})(Si _{2.92} Al _{1.08})O ₁₀ (OH) ₈	PF	—
(Fe _{2.84} Mg _{0.66} Al _{1.91})(Si _{3.29} Al _{0.71})O ₁₀ (OH) ₈	PEL	—
(Fe _{3.18} Mg _{0.75} Al _{1.72})(Si _{2.97} Al _{1.03})O ₁₀ (OH) ₈	PEL	—
(Fe _{3.44} Mg _{0.71} Al _{1.62})(Si _{2.84} Al _{1.16})O ₁₀ (OH) ₈	INF	1.99
(Fe _{3.36} Mg _{0.65} Al _{1.75})(Si _{2.72} Al _{1.28})O ₁₀ (OH) ₈	INF	6.44
(Fe _{3.20} Mg _{0.76} Al _{1.74})(Si _{2.87} Al _{1.13})O ₁₀ (OH) ₈	GC	—
(Fe _{2.71} Mg _{0.75} Al _{2.02})(Si _{3.01} Al _{0.99})O ₁₀ (OH) ₈	GC	—
(Fe _{3.49} Mg _{0.70} Al _{1.60})(Si _{2.87} Al _{1.13})O ₁₀ (OH) ₈	GC	—
(Fe _{3.14} Mg _{0.72} Al _{1.78})(Si _{2.93} Al _{1.07})O ₁₀ (OH) ₈	ave	—
2732 m Burial depth		
(Fe _{3.53} Mg _{0.66} Al _{1.61})(Si _{2.81} Al _{1.19})O ₁₀ (OH) ₈	PF	0.75
(Fe _{3.62} Mg _{0.65} Al _{1.54})(Si _{2.84} Al _{1.16})O ₁₀ (OH) ₈	PEL	—
(Fe _{3.65} Mg _{0.58} Al _{1.57})(Si _{2.81} Al _{1.19})O ₁₀ (OH) ₈	PEL	0.67
(Fe _{3.67} Mg _{0.64} Al _{1.50})(Si _{2.89} Al _{1.11})O ₁₀ (OH) ₈	PEL	0.33
(Fe _{3.68} Mg _{0.69} Al _{1.46})(Si _{2.88} Al _{1.12})O ₁₀ (OH) ₈	PEL	—
(Fe _{3.60} Mg _{0.67} Al _{1.54})(Si _{2.84} Al _{1.16})O ₁₀ (OH) ₈	PEL	6.41
(Fe _{3.23} Mg _{0.70} Al _{1.70})(Si _{3.05} Al _{0.95})O ₁₀ (OH) ₈	GC	0.65
(Fe _{3.57} Mg _{0.66} Al _{1.56})(Si _{2.87} Al _{1.13})O ₁₀ (OH) ₈	ave	—
3878 m Burial depth		
(Fe _{2.98} Mg _{0.91} Al _{1.71})(Si _{3.07} Al _{0.93})O ₁₀ (OH) ₈	PF	1.24
(Fe _{3.08} Mg _{1.05} Al _{1.60})(Si _{2.92} Al _{1.08})O ₁₀ (OH) ₈	PF	2.10
(Fe _{3.14} Mg _{0.99} Al _{1.61})(Si _{2.90} Al _{1.10})O ₁₀ (OH) ₈	PF	—
(Fe _{2.92} Mg _{1.00} Al _{1.76})(Si _{2.87} Al _{1.13})O ₁₀ (OH) ₈	PEL	—
(Fe _{3.45} Mg _{1.01} Al _{1.40})(Si _{2.85} Al _{1.15})O ₁₀ (OH) ₈	INF	—
(Fe _{3.81} Mg _{0.85} Al _{1.29})(Si _{2.81} Al _{1.19})O ₁₀ (OH) ₈	INF	—
(Fe _{3.09} Mg _{1.05} Al _{1.61})(Si _{2.89} Al _{1.11})O ₁₀ (OH) ₈	GC	—
(Fe _{3.29} Mg _{0.98} Al _{1.55})(Si _{2.83} Al _{1.17})O ₁₀ (OH) ₈	GC	—
(Fe _{3.10} Mg _{1.04} Al _{1.61})(Si _{2.90} Al _{1.10})O ₁₀ (OH) ₈	GC	—
(Fe _{3.08} Mg _{1.03} Al _{1.63})(Si _{2.89} Al _{1.11})O ₁₀ (OH) ₈	GC	—
(Fe _{3.03} Mg _{1.05} Al _{1.65})(Si _{2.89} Al _{1.11})O ₁₀ (OH) ₈	GC	—
(Fe _{3.18} Mg _{1.00} Al _{1.58})(Si _{2.91} Al _{1.09})O ₁₀ (OH) ₈	ave	—
4054 m Burial depth		
(Fe _{3.37} Mg _{0.72} Al _{1.65})(Si _{2.88} Al _{1.12})O ₁₀ (OH) ₈	PF	0.46
(Fe _{3.44} Mg _{0.81} Al _{1.57})(Si _{2.81} Al _{1.19})O ₁₀ (OH) ₈	PEL	—
(Fe _{3.42} Mg _{0.80} Al _{1.59})(Si _{2.79} Al _{1.21})O ₁₀ (OH) ₈	PEL	—
(Fe _{3.32} Mg _{0.77} Al _{1.67})(Si _{2.81} Al _{1.19})O ₁₀ (OH) ₈	INF	—
(Fe _{3.74} Mg _{0.69} Al _{1.48})(Si _{2.68} Al _{1.32})O ₁₀ (OH) ₈	GC	—
(Fe _{3.13} Mg _{0.84} Al _{1.73})(Si _{2.88} Al _{1.12})O ₁₀ (OH) ₈	GC	—
(Fe _{3.28} Mg _{0.80} Al _{1.69})(Si _{2.78} Al _{1.22})O ₁₀ (OH) ₈	GC	—
(Fe _{3.60} Mg _{0.77} Al _{1.50})(Si _{2.76} Al _{1.24})O ₁₀ (OH) ₈	RPL	—
(Fe _{3.60} Mg _{0.74} Al _{1.50})(Si _{2.80} Al _{1.20})O ₁₀ (OH) ₈	RPL	—
(Fe _{3.43} Mg _{0.77} Al _{1.60})(Si _{2.80} Al _{1.20})O ₁₀ (OH) ₈	ave	—
4554 m Burial depth		
(Fe _{3.80} Mg _{0.78} Al _{1.37})(Si _{2.73} Al _{1.27})O ₁₀ (OH) ₈	PEL	—
(Fe _{3.29} Mg _{0.87} Al _{1.62})(Si _{2.84} Al _{1.16})O ₁₀ (OH) ₈	PEL	—
(Fe _{3.09} Mg _{1.09} Al _{1.56})(Si _{2.95} Al _{1.05})O ₁₀ (OH) ₈	INF	—
(Fe _{3.31} Mg _{0.98} Al _{1.51})(Si _{2.87} Al _{1.13})O ₁₀ (OH) ₈	INF	—
(Fe _{3.17} Mg _{1.03} Al _{1.57})(Si _{2.92} Al _{1.08})O ₁₀ (OH) ₈	GC	—
(Fe _{3.25} Mg _{1.05} Al _{1.48})(Si _{2.96} Al _{1.04})O ₁₀ (OH) ₈	GC	—
(Fe _{3.16} Mg _{1.14} Al _{1.46})(Si _{3.02} Al _{0.98})O ₁₀ (OH) ₈	GC	—
(Fe _{3.43} Mg _{0.93} Al _{1.48})(Si _{2.84} Al _{1.16})O ₁₀ (OH) ₈	GC	—
(Fe _{3.31} Mg _{0.98} Al _{1.51})(Si _{2.87} Al _{1.13})O ₁₀ (OH) ₈	ave	—

Table 2. Continued.

EDX composition	Texture	% TiO ₂
5470 m Burial depth		
(Fe _{2.85} Mg _{1.19} Al _{1.65})(Si _{2.86} Al _{1.14})O ₁₀ (OH) ₈	PF	—
(Fe _{2.80} Mg _{0.93} Al _{1.87})(Si _{2.92} Al _{1.08})O ₁₀ (OH) ₈	INF	—
(Fe _{2.80} Mg _{1.20} Al _{1.72})(Si _{2.84} Al _{1.16})O ₁₀ (OH) ₈	INF	—
(Fe _{2.91} Mg _{1.13} Al _{1.70})(Si _{2.82} Al _{1.18})O ₁₀ (OH) ₈	GC	—
(Fe _{3.20} Mg _{0.84} Al _{1.75})(Si _{2.66} Al _{1.34})O ₁₀ (OH) ₈	GC	—
(Fe _{2.82} Mg _{1.19} Al _{1.71})(Si _{2.87} Al _{1.13})O ₁₀ (OH) ₈	GC	—
(Fe _{3.36} Mg _{0.86} Al _{1.64})(Si _{2.64} Al _{1.36})O ₁₀ (OH) ₈	GC	—
(Fe _{2.85} Mg _{1.19} Al _{1.65})(Si _{2.86} Al _{1.14})O ₁₀ (OH) ₈	GC	—
(Fe _{2.98} Mg _{1.05} Al _{1.72})(Si _{2.80} Al _{1.20})O ₁₀ (OH) ₈	ave	—

Octahedral Fe Distribution

Fe distribution is slightly asymmetrical, with 12–21% more Fe in 2:1 layer octahedral sheets than hydroxide interlayer octahedral sheets (Figure 5). More Fe in the 2:1 layer implies that Al is somewhat partitioned into the hydroxide interlayer, a finding consistent with other chlorite analyses (Bailey 1988b). The Fe distribution in Tuscaloosa Formation Sp/Ch does not vary or becomes slightly asymmetric with increasing diagenetic grade (Figure 4). Varying the Fe content of interstratified serpentine layers had no measurable effect on 001:003 intensity ratio, so serpentine layers and chlorite layers are assumed to have identical Fe content. This interpretation is consistent with EDX data (see discussion) and has been observed elsewhere for interstratified 7-Å/14-Å minerals (Ahn and Peacor 1985; Jiang et al. 1992; Xu and Veblen 1993).

Occurrence of Titanium

The majority of EDX analyses (77%) showed that TiO₂ comprises <0.3% of Tuscaloosa Formation Sp/Ch, and 40% of the Sp/Ch contained <0.1% TiO₂. However, anatase was detected in all XRD patterns of Tuscaloosa Formation sandstone (Figure 1). The EDX analyses indicating >0.3% were virtually all of Sp/Ch pore-fillings and infillings, suggesting that anatase crystals are intergrown with Sp/Ch in pore space and not near grain contacts. It also implies that Ti does not occur in Tuscaloosa Formation Sp/Ch, a finding consistent with other analyses of chlorite minerals (Curtis et al. 1984; Whittle 1986; Newman 1987; Bailey 1988b; Hillier and Velde 1991; Jiang et al. 1994). Relative XRD peak intensities indicate that the amount of anatase is relatively constant in the <2 μm fraction throughout the Tuscaloosa Formation. The amount of TiO₂ in Tuscaloosa Formation sandstone is 5–10 times higher than what is typically found in sedimentary rocks, and SEM evidence indicates that the anatase formed during early diagenesis following the dissolution of Ti-bearing ultramafic rock fragments. The co-existence of anatase and hematite is indicative of high oxygen fugacity (f_{O₂}) in Tuscaloosa Formation sand-

Table 3. Sp/Ch chemical compositions determined by SEM/EDX, octahedral Fe atoms (per 6 sites) and tetrahedral Al atoms (per 4 sites) as determined by XRD-spacing equations of von Engelhardt (1942) and Brindley (1961), and the *d*-spacings used to estimate Fe and tetrahedral Al.

Burial depth (m)	% <i>Ibb</i>	EDX Composition	XRD Composition spacings			
			Fe ^{VI}	<i>d</i> (060)	Al ^{IV}	<i>d</i> (001)
1937	~100	(Fe _{3.14} Mg _{0.72} Al _{1.78})(Si _{2.93} Al _{1.07})O ₁₀ (OH) ₈	4.14	1.556 Å	1.52	14.11 Å
2732	67	(Fe _{3.57} Mg _{0.66} Al _{1.56})(Si _{2.87} Al _{1.13})O ₁₀ (OH) ₈	3.07	1.551 Å	1.41	14.14 Å
3878	68	(Fe _{3.18} Mg _{1.00} Al _{1.58})(Si _{2.91} Al _{1.09})O ₁₀ (OH) ₈	3.07	1.551 Å	1.44	14.13 Å
4054	70	(Fe _{3.43} Mg _{0.77} Al _{1.60})(Si _{2.80} Al _{1.20})O ₁₀ (OH) ₈	3.07	1.551 Å	1.44	14.13 Å
4554	49	(Fe _{3.31} Mg _{0.98} Al _{1.51})(Si _{2.89} Al _{1.11})O ₁₀ (OH) ₈	2.85	1.550 Å	1.38	14.15 Å
5470	53	(Fe _{2.91} Mg _{1.13} Al _{1.70})(Si _{2.82} Al _{1.18})O ₁₀ (OH) ₈	2.64	1.549 Å	1.34	14.16 Å

stone during early diagenesis (compare Annerston 1968).

DISCUSSION

XRD vs. SEM/EDX Compositional Determinations

The XRD spacings show distinct trends that, based on commonly used XRD-spacing graphs (von Engelhardt 1942; Shirozu 1958; Brindley 1961; Kepezhinskas 1965; Bailey 1972), indicate decreases in octahedral Fe and tetrahedral Al content with increasing temperature. However, the XRD-determined Al and Fe trends observed here are in contrast with commonly observed trends. Temperature-related increases in tetrahedral Al and decreases in octahedral vacancies have been documented in hydrothermal rocks (Cathelineau and Nieva 1985; Cathelineau 1988) and sedimentary rocks (McDowell and Elders 1980; Jahren and Aagard 1989; Hillier and Velde 1991; Jahren and Aagard 1992), and Jahren (1991) and Jahren and Aagard (1992) attributed such changes in chlorite composition to Ostwald ripening-related recrystallization during diagenesis. Increasing Fe content with increasing temperature has been also observed in chlorite in sedimentary rocks, but these changes have been attributed to differences in bulk rock composition (Jahren and Aagard 1992).

XRD determinations of Sp/Ch composition differ significantly from EDX determinations. In the lowest-grade specimen analyzed (1937 m), where Sp/Ch is the *Ibb* polytype, the XRD estimate of Fe content is approximately 30% greater than the EDX value, and tetrahedral Al (XRD estimate) is approximately 40% higher than the EDX value. In the highest-grade specimen analyzed (5470 m), where the polytype is mixed-layer *Ibb/Iaa* with 47% *Iaa*, XRD estimates of octahedral Fe and tetrahedral Al are closer to the EDX values but still differ by 9% (Fe) to 14% (Al) (Table 3).

We conclude that the apparent XRD-determined trends are erroneous and actually record changes in cell dimensions related to polytype transformations. The *a* and *b* cell dimensions of the *Iaa* structure (5.330 and 9.294 Å) are less than the corresponding cell dimensions of the *Ibb* structure (5.340 and 9.336 Å), and the *c** dimension of *Iaa* is greater than that of *Ibb* (14.31 vs. 14.11 Å). The transformation of the *Ibb* polytype to *Iaa* occurs progressively through a series of mixed-layer *Ibb/Iaa* proportions, and the *d*-spacings used to estimate chemical composition progressively change with the polytype transformation (Table 3). The apparent trend of decreasing tetrahedral Al actu-

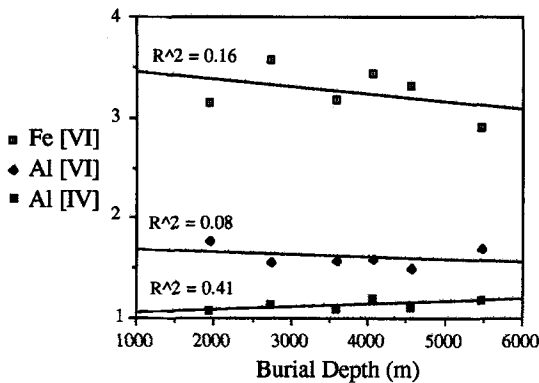


Figure 4. SEM/EDX determinations of tetrahedral Al (Al^{IV}), octahedral Al (Al^{VI}), and octahedral Fe (Fe^{VI}) plotted vs. burial depth. Each point represents the mean of 8–11 individual analyses as shown in Table 2.

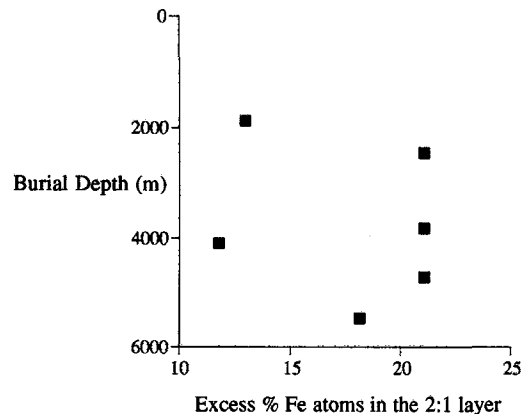


Figure 5. The distribution of Fe atoms between the 2:1 layer and the hydroxide interlayer as estimated by comparing analytical XRD patterns with NEWMOD-calculated XRD patterns (Reynolds 1985).

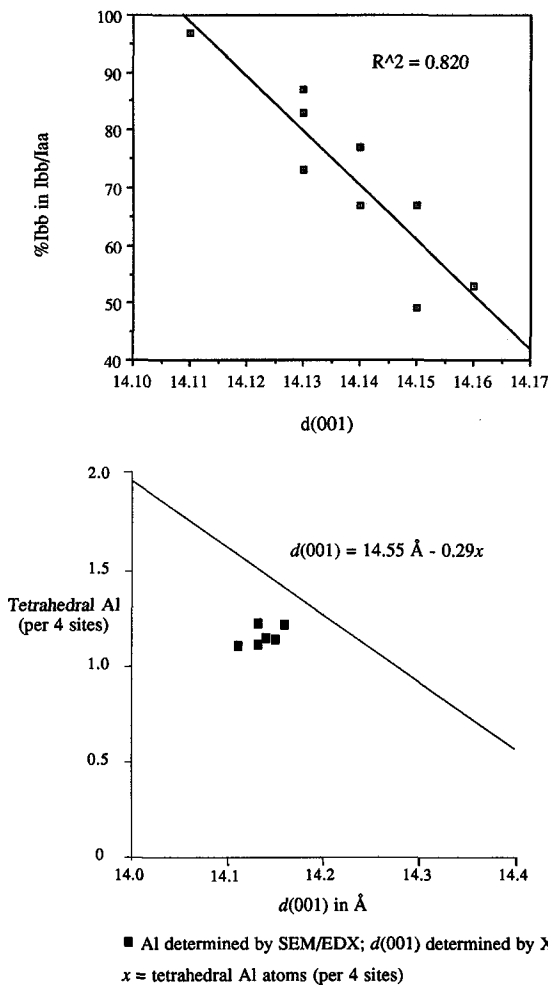


Figure 6a. The relationship between Sp/Ch polytypism (% Ibb layers in Ibb/Iaa) and $d(001)$.

Figure 6b. Tetrahedral Al content (as determined by SEM/EDX) plotted against the regression line of Brindley (1961).

ally reflects the difference in the c^* dimension between the Ibb and Iaa polytypes (Figure 6), and the apparent decrease in Fe is attributed to differences in the a and b dimensions between the Ibb and Iaa polytypes (Figure 7). Using d -spacing equations determined by Shirouzu (1958) and Kepezhinskas (1965) also gives the same erroneous trends. It is apparent from this study and that of Whittle (1986) that, while d -spacing equations may be applicable to Ibb chlorite, they must be used with caution when examining type-I chlorite, particularly where polytype transformations have occurred.

The Lack of Compositional Variation

Perhaps the most intriguing aspect of Tuscaloosa Formation serpentine/chlorite is that, in spite of continuous diagenetic mineralogical reactions, the Sp/Ch

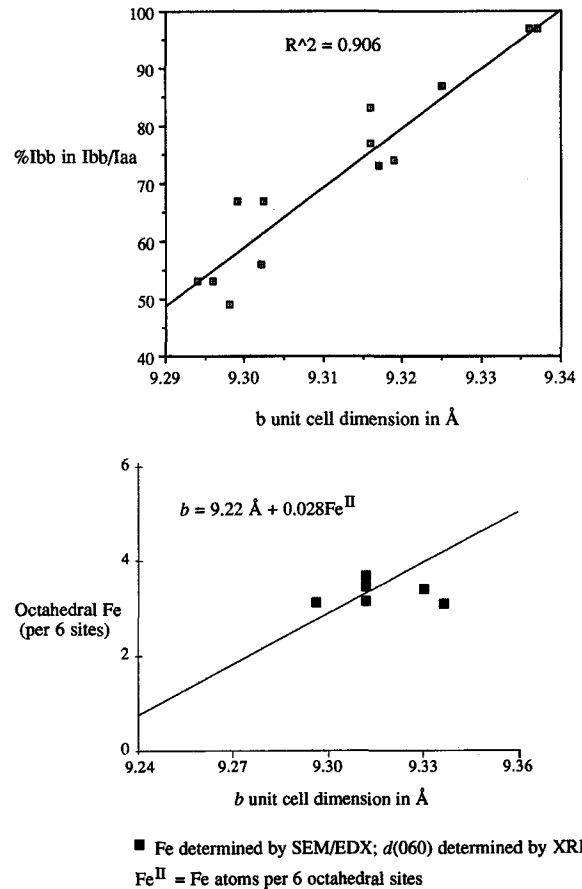


Figure 7a. The relationship between Sp/Ch polytypism (% Ibb layers in Ibb/Iaa) and $d(010)$.

Figure 7b. Octahedral Fe content (as determined by SEM/EDX) plotted against the regression line of von Engelhardt (1942).

exhibits very little compositional variation. Typically, chlorite minerals respond to increasing diagenetic grade by undergoing changes in chemical composition, particularly decreases in Si, octahedral Al and octahedral vacancies, and related increases in tetrahedral Al, total Al and octahedral occupancy. These changes are consistent with progression toward metamorphic chlorite compositions (McDowell and Elders 1980; Hillier and Velde 1991; Jahren and Aagaard 1992; de Caritat et al. 1993; Hillier 1994). For example, Jahren and Aagaard (1992) observed relatively progressive increases with increasing temperature (90 to 180 °C) in Fe (2.4 to 4.1 atoms pfu) and in tetrahedral Al (0.9 to 1.3 atoms pfu) combined with decreasing octahedral vacancies (0.4 to 0.1 sites pfu). Conversely, in Tuscaloosa Formation Sp/Ch, Fe, Mg, octahedral vacancies, octahedral Al and total Al exhibit significantly less range and no distinctive systematic variation as a function of burial depth (Table 3; Figure 4). The only parameter that exhibits a statisti-

cally significant trend is the slight increase in tetrahedral Al (Figure 4), the magnitude of which is much less than observed by, for example, Jahren and Aagaard (1992) and Hillier (1994). Jahren (1991), Jahren and Aagaard (1992) and Hillier (1994) have attributed the progressive changes in composition to re-equilibration of chlorite during prograde Ostwald-ripening crystal growth, whereby fine-grained crystals dissolve and precipitate on coarser crystals. However, mean crystallite thickness (c^* direction) and crystal size of Tuscaloosa Formation Sp/Ch do not vary with temperature (Thomsen 1982; Ryan and Reynolds 1996), and the serpentine-to-chlorite and *Ibb-to-Iaa* reactions appear to involve no crystal growth. The mineralogic reactions most likely occur on a layer-by-layer basis, with individual layers dissolving and reprecipitating within coherent crystallites, a conclusion that is consistent with similar findings obtained by HRTEM analyses of mixed-layer berthierine/chlorite (Xu and Veblin 1993). Additionally, the lack of dissolution-precipitation crystal growth may have prevented the Sp/Ch cations from being mobile enough to undergo major exchange with pore water during the mineralogic reactions. A plausible reason for the lack of Ostwald-ripening crystal growth is that the Sp/Ch crystals are of approximately uniform size (Thomsen 1982), and thus there was no driving mechanism for Ostwald ripening (Eberl et al. 1990). The lack of compositional variation may invite the suggestion that pore water composition was consistent throughout the interval studied, but the progressive transformation of hematite to pyrite and the disappearance of kaolin with increasing depth indicates that pore water composition was not constant.

It is interesting that Sp/Ch in the Tuscaloosa Formation responded to increasing grade not by changing composition, as is the case in many natural systems (Cathelineau and Nieva 1985; Hillier and Velde 1991; Jahren and Aagaard 1992; de Caritat et al. 1993), but by the pathway of altering to higher-temperature structures without changing composition (Nelson and Roy 1958; Brown and Bailey 1962; Jiang et al. 1992). We interpret the lack of compositional variation as indicating that the serpentine-to-chlorite and *Ibb-to-Iaa* reactions described here are isochemical and perhaps largely controlled by temperature.

Octahedral Occupancy

Octahedral vacancies were found in all Tuscaloosa Formation Sp/Ch samples, but the cause of these vacancies is uncertain. They may be related to dioctahedral substitutions or to analytical errors (Hillier 1994; Jiang et al. 1994). Hillier and Velde (1991) indicated that excess Al is due to high Si:Al ratios common to diagenetic chlorites as compared to metamorphic chlorites, which commonly have no octahedral vacancies (Laird 1988). In diagenetic and hy-

drothermal systems, octahedral vacancies have been observed to decrease with increasing grade, possibly indicating a progression toward metamorphic chlorite (Cathelineau and Nieva 1985; Hillier and Velde 1991; Jahren and Aagaard 1992; de Caritat et al. 1993). However, in a recent review of chlorite geothermometry, Jiang et al. (1994) indicate that most octahedral vacancies in chlorite are caused by inclusions of other minerals, and decreasing octahedral vacancies with increasing grade are attributed to decreases of mixed layers or inclusions as minerals become more homogeneous with increasing grade.

There appears to be no correlation between octahedral vacancies and burial depth in Tuscaloosa Formation Sp/Ch, a finding that is consistent with the overall lack of compositional variation in the Sp/Ch. It also indicates that 1) Tuscaloosa Formation Sp/Ch undergoes mineralogic transformations by a reaction mechanism different from that of many chlorites (Cathelineau and Nieva 1985; Hillier and Velde 1991; Jahren and Aagaard 1992), and/or 2) Sp/Ch does not contain inclusions that give possibly erroneous trends in octahedral occupancy.

Composition of the Serpentine Layers

The chemical composition of serpentine-like layers appears to be similar or identical to chlorite layers in Tuscaloosa Formation Sp/Ch. The evidence for this is that the composition of Sp/Ch with 21% Sp layers is nearly identical to the composition of Sp/Ch with only 3% Sp layers. If the Sp and Ch layers were to differ significantly in composition, the compositions of Sp(.21)/Ch and Sp(.03)/Ch would also be expected to differ. This approach was also used in an analytical electron microscopy (AEM) study of Gulf Coast shales by Ahn and Peacor (1985), and they also found that the chemical compositions of interstratified 7-Å serpentine-like layers and 14-Å chlorite layers were nearly identical. Jiang et al. (1992), Xu and Veblin (1993) and Bailey et al. (1995) have also observed interstratified 7-Å/14-Å minerals with 7-Å and 14-Å layers that have nearly identical compositions.

The composition of Tuscaloosa Formation Sp/Ch (and therefore, presumably, Sp layers) is very similar to chemical compositions of berthierine as reviewed by Brindley (1982) and of mixed-layer berthierine/chlorite examined by Ahn and Peacor (1985). Sp/Ch and berthierine respond similarly to increasing temperature, with berthierine transforming to chlorite (Iijima and Matsumoto 1982) and Sp/Ch transforming to end-member chlorite via a mixed-layer series (Walker and Thompson 1990; Hillier 1994; Ryan and Reynolds 1996), although it is not known whether or not berthierine transforms to chlorite via a mixed-layer series in sedimentary rocks (Velde et al. 1974; Iijima and Matsumoto 1982; Hornibrook and Longstaffe 1996). The similarity in structure (Sp and berthierine are both

7-Å phases) and composition between Sp/Ch and berthierine implies that they form under similar geochemical conditions (Hillier 1994), but differences in particle morphology and host rock suggest they have different origins. Berthierine commonly occurs as concentric ooids in ancient ironstones (Bailey 1988b; Velde 1989) and often originates by reaction of siderite with kaolin (James 1966; Iijima and Matsumoto 1982), whereas Sp/Ch occurs as pore-linings, peloids and infillings in tropical marine sandstones and may originate as odinite (Ehrenberg 1993; Hillier 1994; Ryan and Reynolds 1996), a 7-Å Fe-rich mineral that forms at the sediment-seawater interface (Bailey 1988a; Odín 1990). It is primarily because of the differences in particle morphology and host rock type that we refer to the 7-Å layers in Sp/Ch as serpentine rather than the more specific mineral name berthierine.

The Relationship of Titanium, Chlorite and Anatase

TiO₂, occurring as anatase, is an important component of Tuscaloosa Formation sandstone, yet its abundance and origin are uncertain. Biotite commonly contains 1–2% TiO₂ with values ranging as high as 9% (Whitney and McClelland 1983; Newman 1987; Brigatti et al. 1991; Deer et al. 1992), and Fe-Mg silicates in the pyroxene and amphibole groups can tolerate up to 10% TiO₂, but chlorite and Sp/Ch typically contain no Ti. Guidotti (1984), Eggleton and Banfield (1985), Otten and Buseck (1987), Guidotti (1984), Abrecht and Hewitt (1988) and Brigatti et al. (1991) report that Ti occurs as Ti⁴⁺ in biotite octahedral sites, which then raises the question: why does Ti not occur in chlorite octahedral sites? Three possible explanations for the lack of Ti in chlorite minerals are discussed below.

High Charges of Ti⁴⁺ and Al³⁺

The high charges of Ti⁴⁺ and Al³⁺ suggest that large amounts of either, or both, in octahedral sheets would lead to localized concentrations of high charge, vacancies or charge imbalances resulting from exchange reactions such as TiMg₋₂ and Al₂Mg₋₃. The incompatibility of Ti and Al in biotite octahedral sheets was demonstrated by Labotka (1983), who noted a strong inverse correlation between octahedral Al and Ti in metamorphic biotite and indicated that Ti^{VI} and Al^{VI} are related by the charge-balanced substitution:



Biotite with >0.4 Al (per 3 sites) contained no Ti, and biotite with >0.3 Ti contained no Al^{VI}. Compositions given by Whitney and McClelland (1983) and Guidotti (1984) also indicate an inverse correlation between octahedral Al and Ti. Furthermore, comparison of biotite and chlorite compositions shows that while biotite can contain up to 9% TiO₂, chlorite contains little or no Ti (typically well less than 0.2% TiO₂). Chlorite routinely contains at least twice as much Al per octahedral sheet

as does biotite, with the high amounts of octahedral Al being necessary for 1) electrostatic bonding between the hydroxide interlayer and the 2:1 layer and 2) neutralization of negative charge on the tetrahedral sheets. Shirozu (1980) has demonstrated that considerable Al can substitute into the 2:1 octahedral sheet as well as the interlayer octahedral sheet of chlorite (Bailey 1988b), and this is an important point because it provides a mechanism for exclusion of Ti from both octahedral sheets in chlorite. Thus, the incompatibility of Ti and Al in octahedral sheets, combined with high octahedral Al common to chlorite, appears to be a valid explanation for the lack of Ti in chlorite and Sp/Ch.

Oxygen Fugacity and the Stability of TiO₂

The presence of anatase throughout the Tuscaloosa Formation may indicate that the most stable occurrence of Ti in diagenetic environments is as an oxide rather than as a cation in silicates. Evidence for this theory is based on studies of Ti and biotite in metamorphic rocks. For example, Annerston (1968) studied a metamorphosed iron-formation and determined that Ti occurs as an oxide in environments with high oxygen fugacity, but as a component of silicates (such as biotite and amphibole) at low oxygen fugacity. Additional studies of metamorphic and synthetic biotite also indicate that Ti content in biotite is inversely proportional to oxygen fugacity (Bachinski and Simpson 1984; Patino Douce 1993) as well as directly proportional to temperature (Forbes and Flower 1974; Guidotti et al. 1977; Monier and Robert 1986; Abrecht and Hewitt 1988). High oxygen fugacity and low temperature in many diagenetic environments may explain the abundance of anatase, but it does not sufficiently explain the lack of Ti in chlorite because, in systems where biotite and chlorite coexist under similar *f*_{O₂} and temperature conditions, biotite contains 10 times more Ti than coexisting chlorite (compare Guidotti et al. 1977; Labotka 1983).

Differences in Unit-Cell Characteristics between Biotite and Chlorite

The *a* and *b* unit-cell dimensions of biotite and chlorite are nearly identical, and the radii of Ti³⁺ (0.68) and Ti⁴⁺ (0.76) are very similar to the ionic radii of Fe and Mg between 0.64 and 0.74 (Deer et al. 1992), so it is unlikely that the sizes of ionic radii or differences in octahedral sites between biotite and chlorite can explain the lack of Ti in chlorite. Interlayer differences between biotite and chlorite also seem insufficient to explain the Ti problem. The interlayers differ in that the chlorite interlayer comprises metal cations bonded to octahedrally coordinated hydroxyls that maintain hydrogen bonds with basal oxygens of adjacent tetrahedral sheets, whereas biotite contains interlayer K atoms in 12-fold coordination with basal tetrahedral oxygens. However, in both minerals, the

octahedral sheet in the 2:1 layer is separated from the interlayer by a tetrahedral sheet, and this factor, combined with the relatively large distance between octahedral cations and the interlayer ($\sim 5 \text{ \AA}$), makes it unlikely that interlayer differences could explain the lack of Ti.

The lack of Ti in chlorite minerals appears to be best explained by the high octahedral Al content of chlorite minerals. Octahedral Al in chlorite is necessary for electrostatic bonding and charge neutralization, but its presence creates an environment that prohibits inclusion of the highly charged Ti^{4+} . This phenomenon is particularly evident in biotite, where octahedral Ti and tetrahedral Al are inversely correlated. The highly oxidizing conditions common in diagenetic environments may also affect Ti partitioning because, at high f_{O_2} , Ti is most stable as anatase (Annerston 1968).

The Origin of Anatase in the Tuscaloosa Formation

The high concentrations of TiO_2 in Tuscaloosa Formation sandstone probably reflect the abundance of Ti-bearing ultramafic rock fragments throughout the Tuscaloosa Formation. Ultramafic detrital clasts are ubiquitous in the Tuscaloosa Formation, having been sourced from contemporaneous volcanic centers in the circum-Gulf Coast region (Hunter and Davies 1979; Thomsen 1982). The extremely low mobility of Ti in aqueous environments implies that the Ti was not imported by fluids, and the most plausible source for the Ti is breakdown of Ti-bearing minerals in the volcanic clasts during early diagenesis (Morad 1986).

We conclude that, during the earliest stages of diagenesis, detrital Ti-bearing mafic clasts dissolved (Thomsen 1982) and the dissolution products crystallized as odinite (Ryan and Reynolds 1996), a short-lived precursor to chlorite that forms within the upper decimeter of sediment in tropical marine environments (Bailey 1988a; Odin 1990). This proposed origin of odinite is significant in that it differs from observed modern origins, which are characterized by their proximity to Fe-rich tropical river water (Bailey 1988a; Odin 1990). However, it is likely that, given a conducive postdepositional environment (Bailey 1988a), the geochemical conditions within pores and cavities would favor odinite formation regardless of the Fe source. Odinite is poorly crystalline and contains low octahedral Al (Bailey 1988a, 1988b), so it could have contained Ti in octahedral sites. The occurrence of high amounts of TiO_2 in the central part of pores (intermixed with Sp/Ch peloids, pore-fillings and infillings), and its rare occurrence in pore-linings (it occurs locally in the outermost portion of the pore-lining), implies that anatase formed during the latter stages of Sp/Ch crystallization. Thus, when odinite transformed to Sp/Ch in the upper few meters of sediment (Bailey 1988a; Ehrenberg 1993; Hillier 1994; Ryan and Reyn-

olds 1996), Ti was not incorporated into Sp/Ch due to the high amounts of octahedral Al in Sp/Ch. The liberated Ti crystallized as anatase proximal to Sp/Ch peloids and infillings, and the newly formed Sp/Ch pore-linings included only traces of anatase.

CONCLUSIONS

- 1) XRD-determined d -spacings do not accurately estimate Sp/Ch composition, primarily because Sp/Ch d -spacings progressively change during *Ibb/Iaa* polytype reactions, creating erroneous compositional trends.
- 2) The lack of significant compositional changes in Sp/Ch with increasing diagenetic grade reflects layer-by-layer (cell-preserved) mineralogic reactions and the lack of Ostwald-ripening crystal growth.
- 3) Chlorite minerals, including Sp/Ch, lack Ti due to high concentrations of octahedral Al^{3+} that prohibit inclusion of the highly charged Ti^{4+} .
- 4) Anatase formed in an oxidizing environment when Ti was liberated during the formation of Sp/Ch from precursor Ti-bearing detrital minerals via the short-lived intermediate phase odinite.

ACKNOWLEDGMENTS

We gratefully acknowledge a thorough review by S. Hillier, as well as editorial handling by W. Hudnall and R. Ferrell. J. Moe helped to inspire the idea for this paper and reviewed an early version. Conversations with L. Stem regarding chlorite crystal chemistry were also very helpful. C. Daghlian of the Dartmouth College electron microscope laboratory provided assistance with SEM/EDX analyses, as did J. Blum and M. Brown. We wish to thank D. R. Pevear and Exxon Production Research Company, Houston, Texas, for financial support and for core samples.

REFERENCES

- Abrecht J, Hewitt DA. 1988. Experimental evidence on the substitution of Ti in biotite. *Am Mineral* 73:1275-1284.
- Ahn JH, Peacor DR. 1985. Transmission electron microscopic study of diagenetic chlorite in Gulf Coast argillaceous sediments. *Clays Clay Miner* 33:228-237.
- Al-Dahan AA, Morad S. 1986. Chemistry of detrital biotites and their phyllosilicate intergrowths in sandstones. *Clays Clay Miner* 34:539-548.
- Alford EV. 1983. Compositional variations of authigenic chlorites in the Tuscaloosa Formation, Upper Cretaceous of the Gulf Coast Basin [M.S. thesis]. New Orleans, LA:Univ. of New Orleans.
- Annerston H. 1968. A mineral chemical study of a metamorphosed iron formation in northern Sweden. *Lithos* 1: 374-397.
- Bachinski SW, Simpson EL. 1984. Ti-phlogopites of the Shaw's Cove Minette: A comparison with micas of other lamprophyres, potassic rocks, kimberlites and mantle xenoliths. *Am Mineral* 69:41-56.
- Bailey SW. 1972. Determination of chlorite compositions by X-ray spacings and intensities. *Clays Clay Miner* 20:381-388.
- Bailey SW. 1988a. Odinite, a new dioctahedral-trioctahedral Fe^{3+} -rich 1:1 clay mineral. *Clay Miner* 23:237-247.

- Bailey SW. 1988b. Chlorites: Structures and crystal chemistry. In: Bailey SW, editor. *Hydrous phyllosilicates (exclusive of micas)*, Rev Mineral 19. Washington, DC: Mineral Soc Am. p 347–403.
- Bailey SW, Banfield JF, Barker WW. 1995. Dozyite, a 1:1 regular interstratification of serpentine and chlorite. *Am Mineral* 80:65–77.
- Brigatti MF, Poppi L, Fabbri A. 1991. Corrensites: genetic relationships assessed by multivariate statistical analysis. *Bull Mineral* 109:543–553.
- Brindley GW. 1961. Chlorite minerals. In: Brown G, editor. *The X-ray identification and crystal structures of clay minerals*. London: Mineral Soc. p 242–296.
- Brindley GW. 1982. Chemical composition of berthierines—A review. *Clays Clay Miner* 30:153–155.
- Brown G, Bailey SW. 1962. Chlorite polytypism: I. Regular and semi-random one-layer structures. *Am Mineral* 47: 819–850.
- Cathelineau M. 1988. Cation site occupancy in chlorites and illites as a function of temperature. *Clay Miner* 23:471–485.
- Cathelineau M, Nieve D. 1985. A chlorite solid solution geothermometer: The Los Azufres (Mexico) geothermal system. *Contrib Mineral Petrol* 91:235–244.
- Chagnon A, Desjardins M. 1991. Determination de la composition de la chlorite par diffraction et microanalyse aux rayons X. *Can Mineral* 29:245–254.
- Curtis CD, Ireland BJ, Whiteman JA, Mulvaney R, Whittle CK. 1984. Authigenic chlorites: Problems with chemical analysis and structural formula calculation. *Clay Miner* 19:471–481.
- de Caritat P, Hutcheon I, Walshe JL. 1993. Chlorite geothermometry: A review. *Clays Clay Miner* 41:219–239.
- Deer WA, Howie RA, Zussman J. 1992. *An introduction to the rock-forming minerals*, 2nd ed. New York: J Wiley. 696 p.
- Eberl DD, Srodon J, Kralik M, Taylor BE, Peterman ZE. 1990. Ostwald ripening of clays and metamorphic minerals. *Science* 248:474–477.
- Eggleton RA, Banfield JF. 1985. The alteration of granitic biotite to chlorite. *Am Mineral* 70:902–910.
- Ehrenberg SN. 1993. Preservation of anomalously high porosity in deeply buried sandstones by grain-coating chlorite examples from the Norwegian Continental Shelf. *Am Assoc Petrol Geol Bull* 77:1260–1286.
- von Engelhardt W. 1942. Die Strukturen von Thuringit, Bavalit, und Chamosit und ihre Stellung in der Chloritgruppe. *Z Kristallogr* 104:142–159.
- Forbes WC, Flower MFJ. 1974. Phase relations of titanophlogopite, $K_2Mg_4TiAl_2Si_6O_{20}(OH)_4$: A refractory phase in the upper mantle? *Earth Planet Sci Lett* 22:60–66.
- Foster MD. 1962. Interpretation of the composition and a classification of the chlorites. *US Geol Survey Prof Paper* 414-A:1–33.
- Guidotti CV. 1984. Micas in metamorphic rocks. In: Bailey SW, editor. *Micas*, Rev Mineral 13. Washington, DC: Mineral Soc Am. p 357–467.
- Guidotti CV, Cheney JT, Guggenheim S. 1977. Distribution of titanium between coexisting muscovite and biotite in pelitic schists from Northwestern Maine. *Am Mineral* 62: 438–448.
- Hamlin KH, Cameron CP. 1987. Sandstone petrology and diagenesis of Lower Tuscaloosa Formation reservoirs in the McComb and Little Creek field areas, southwest Mississippi. *Trans Gulf Coast Assoc Geol Soc* 37:95–104.
- Heald MT, Anderegg RC. 1960. Differential cementation in the Tuscarora sandstone. *J Sed Petrol* 30:568–577.
- Hearne JH, Lock BE. 1985. Diagenesis of the Lower Tuscaloosa as seen in the DuPont de Nemours #1 Lester Earnest, Harrison County, Mississippi. *Trans Gulf Coast Assoc Geol Soc* 35:387–393.
- Hillier S. 1994. Pore-lining chlorites in siliciclastic reservoir sandstones: Electron microscope, SEM, and XRD data, and implications for their origin. *Clay Miner* 29:665–679.
- Hillier S, Velde B. 1991. Octahedral occupancy and chemical composition of diagenetic (low-temperature) chlorites. *Clay Miner* 26:149–168.
- Hogg MD. 1988. Newtonia Field: A model for mid-dip Lower Tuscaloosa retrograde deltaic sedimentation. *Trans Gulf Coast Assoc Geol Soc* 38:461–471.
- Hornibrook ERC, Longstaffe FJ. 1996. Berthierine from the Lower Cretaceous Clearwater Formation, Alberta, Canada. *Clays Clay Miner* 44:1–21.
- Hunter BE, Davies DK. 1979. Distribution of volcanic sediments in the Gulf Coast Province—Significance to petroleum geology. *Trans Gulf Coast Assoc Geol Soc* 29:147–155.
- Iijima A, Matsumoto R. 1982. Berthierine and chamosite in coal measures of Japan. *Clays Clay Miner* 30:264–274.
- Jahren JS. 1991. Evidence of Ostwald ripening related recrystallization of diagenetic chlorites from reservoir rocks offshore Norway. *Clay Miner* 26:169–178.
- Jahren JS, Aagaard P. 1989. Compositional variations in diagenetic chlorites and illites, and their relationships with formation water chemistry. *Clay Miner* 24:157–170.
- Jahren JS, Aagaard P. 1992. Diagenetic illite-chlorite assemblages in arenites: I. Chemical evolution. *Clays Clay Miner* 40:540–546.
- James HL. 1966. Chemistry of the iron-rich sedimentary rocks. *US Geol Survey Prof Paper* 440-W. 60 p.
- Jiang W-T, Peacor DR, Buseck PR. 1994. Chlorite geothermometry?—Contamination and apparent octahedral vacancies. *Clays Clay Miner* 42:593–605.
- Jiang W-T, Peacor DR, Slack JF. 1992. Microstructures, mixed-layering, and polymorphism of chlorite and retrograde berthierine in the Kidd Creek massive sulfide deposit, Ontario. *Clays Clay Miner* 40:501–514.
- Kepezhinskas KB. 1965. Composition of chlorites as determined from their physical properties. *Dokl Akad Nauk S.S.S.R, Earth Sci Sect* 164:126–129 (English).
- Labotka TC. 1983. Analysis of the compositional variation of biotite in pelitic hornfelses from Northeastern Minnesota. *Am Mineral* 68:900–914.
- Laird J. 1988. Chlorites: *Metamorphic petrology*. In: Bailey SW, editor. *Hydrous phyllosilicates (exclusive of micas)*, Rev Mineral 19. Washington, DC: Mineral Soc Am. p 405–447.
- Li G, Peacor DR. 1993. Sulfides precipitated in chlorite altered from detrital biotite: A mechanism for local sulfate reduction? *Abstr Progr Geol Soc Am Annu Meet* 25:146–147.
- McDowell SM, Elders WA. 1980. Authigenic layer silicate minerals in borehole Elmore #1, Salton Sea Geothermal Field California. *Contrib Mineral Petrol* 74:293–310.
- Monier G, Robert JL. 1986. Titanium in muscovites from two mica granites: Substitutional mechanism and partition with coexisting biotites. *Neues Jahrbuch fuer Mineralogie, Abhandlungen* 153:147–161.
- Morad S. 1986. SEM Study of authigenic rutile, anatase, and brookite in Proterozoic sandstones from Sweden. *Sed Geol* 46:77–89.
- Nelson BW, Roy R. 1958. Synthesis of the chlorites and their structural and chemical constitution. *Am Mineral* 43:707–725.
- Newman ACD. 1987. *Chemistry of clays and clay minerals*. New York: J Wiley. 480 p.

- Odin GS. 1990. Clay mineral formation at the continent-ocean boundary: The verdine facies. *Clay Miner* 25:477-483.
- Otten MT, Buseck PR. 1987. TEM study of the transformation of augite to sodic pyroxene in eclogitized ferrogabbro. *Contrib Mineral Petrol* 96:529-538.
- Patino Douce AE. 1993. Titanium substitution in biotite: An empirical model with applications to thermometry, O₂ and H₂O barometries, and consequences for biotite stability. *Chem Geol* 108:133-162.
- Pittman ED, Lumsden DN. 1968. Relationship between chlorite coatings on quartz grains and porosity, Spiro Sand, Oklahoma. *J Sed Petrol* 38:668-670.
- Reynolds RC Jr. 1985. NEWMOD—A computer program for the calculation of one-dimensional diffraction profiles of clays. Hanover, New Hampshire: RC Reynolds, Jr, 8 Brook Road.
- Reynolds RC Jr, DiStefano MP, Lahann RW. 1992. Randomly interstratified serpentine/chlorite: Its detection and quantification by powder X-ray diffraction methods. *Clays Clay Miner* 40:262-267.
- Ryan PC. 1994. Serpentine/chlorite and illite/smectite in the Tuscaloosa Formation: Origins, chemistry, mineralogic structures, and oxygen isotope compositions [Ph.D. thesis]. Hanover, NH: Dartmouth College. 177 p.
- Ryan PC, Reynolds RC Jr. 1996. The origin and diagenesis of grain-coating serpentine-chlorite in Tuscaloosa Formation sandstone, U.S. Gulf Coast. *Am Miner* 81:213-225.
- Schulze DG. 1982. The identification of soil iron oxide minerals by differential X-ray diffraction. *Soil Sci Soc Am J* 45:437-440.
- Shirozu H. 1958. X-ray powder and cell dimensions of some chlorites in Japan, with a note on their interference colors. *Mineral J (Jpn)* 2:209-223.
- Shirozu H. 1980. Cation distribution, sheet thickness, and O-OH space in trioctahedral chlorites—An X-ray and infrared study. *Mineral J (Jpn)* 10:14-34.
- Stancliffe RJ, Adams ER. 1986. Lower Tuscaloosa fluvial channel styles at Liberty Field, Amite County, Mississippi. *Trans Gulf Coast Assoc Geol Soc* 36:305-313.
- Thomsen A. 1982. Preservation of porosity in the Deep Woodbine/Tuscaloosa Trend, Louisiana. *J Petrol Technol* 34:1156-1162.
- Velde B. 1989. Phyllosilicate formation in berthierine peloids and iron oolites. In: Young TP, Taylor WEG, editors. *Phanerozoic ironstones*. London: Geol Soc Spec Publ 46. p 3-8.
- Velde B, Raoult J-F, Leikine M. 1974. Metamorphosed berthierine pellets in mid-Cretaceous rocks from north-eastern Algeria. *J Sed Petrol* 44:1275-1280.
- Walker JR, Hluchy MM, Reynolds RC Jr. 1988. Estimation of heavy atom content and distribution in chlorite using corrected X-ray powder diffraction intensities. *Clays Clay Miner* 36:359-364.
- Walker JR, Thompson GR. 1990. Structural variations in illite and chlorite in a diagenetic sequence from the Imperial Valley, California. *Clays Clay Miner* 38:315-321.
- Whitney PR, McClelland JM. 1983. Origin of biotite-hornblende-garnet coronas between oxides and plagioclase in olivine metagabbros, Adirondack Region, New York. *Contrib Mineral Petrol* 82:34-41.
- Whittle CK. 1986. Comparison of sedimentary chlorite compositions by X-ray diffraction and analytical TEM. *Clay Miner* 21:937-947.
- Wiygul GJ, Young LM. 1987. A subsurface study of the Lower Tuscaloosa Formation at Olive Field, Pike and Amity Counties, Mississippi. *Trans Gulf Coast Assoc Geol Soc* 37:295-302.
- Yau YC, Peacor DR, Essene EJ. 1987. Authigenic anatase and titanite in shales from the Salton Sea geothermal field, California. *Neues Jahrbuch fuer Mineralogie, Monatshefte* 10:441-452.
- Yoneyama H, Haga S, Yamanaka S. 1989. Photocatalytic activities of microcrystalline TiO₂ incorporated in sheet silicates of clay. *J Phys Chem* 93:4833-4837.
- Xu H, Veblen DR. 1993. Periodic and disordered interstratification and other microstructures in the chlorite-berthierine series [abstract]. *Abstr Progr Geol Soc Am Annu Meet* 25:146.

(Received 17 July 1995; accepted 3 July 1996; Ms. 2671)